



## Special Feature: Powertrain and Environment

*Research Report*

### Low Emissions and High-efficiency Diesel Combustion Using Highly Dispersed Spray with Restricted In-cylinder Swirl and Squish Flows

Kazuhisa Inagaki, Jun'ichi Mizuta, Takayuki Fuyuto, Takeshi Hashizume, Hirokazu Ito, Hiroshi Kuzuyama, Tsutomu Kawae and Masaaki Kono

*Report received on Mar. 26, 2013*

■ **ABSTRACT** ■ A new clean diesel combustion concept has been proposed and its excellent performance with respect to gas emissions and fuel economy were demonstrated using a single cylinder diesel engine. It features the following three items: (1) low-penetrating and highly dispersed spray using a specially designed injector with very small and numerous orifices, (2) a lower compression ratio, and (3) drastically restricted in-cylinder flow by means of very low swirl ports and a lip-less shallow dish type piston cavity.

Item (1) creates a more homogeneous air-fuel mixture with early fuel injection timings, while preventing wall wetting, i.e., impingement of the spray onto the wall. In other words, this spray is suitable for premixed charge compression ignition (PCCI) operation, and can decrease both nitrogen oxides (NO<sub>x</sub>) and soot considerably when the utilization range of PCCI is maximized.

However, in diffusive combustion, especially at full load, a low-penetrating spray potentially causes higher soot emissions and results in lower maximum torque. In this case, item (2) is applied to recover full-load performance. The lower compression ratio enables diffusive combustion phasing to be advanced more with an earlier injection timing because of a larger margin between the compression-end pressure and the allowable maximum in-cylinder pressure. This results in lower soot emissions because enough time is created to oxidize soot before the end of the combustion period.

A lower compression ratio often leads to worse cold-condition engine performance aspects, such as cold startability, unburned hydrocarbons, and white smoke. Item (3) is applied to compensate for such practical problems. Drastically weakened in-cylinder flow keeps the compression-end temperature to the same level as a conventional engine with an ordinary compression ratio by decreasing heat-flux escaping through the chamber wall (i.e., heat-loss).

Although a weak in-cylinder gas motion might lead to higher soot emissions due to slower fuel-air mixing, it should be noted that the highly dispersed spray of item (1) enables PCCI-dominant combustion in which the fuel-air mixing process is less dependent on in-cylinder flow.

In this way, these three items act mutually to compensate for each other's drawbacks, while maximizing their advantages. Consequently, NO<sub>x</sub> emissions in the New European Driving Cycle (NEDC) can be reduced drastically to less than 1/4 of the level of a conventional engine, or less than half of the Euro 6 standard without deteriorating fuel consumption, full-load torque, or cold-condition performance.

■ **KEYWORDS** ■ Heat Engine, Compression Ignition Engine, Economy, Efficiency, HCCI

#### 1. Introduction

Carbon dioxide (CO<sub>2</sub>) is becoming a world-wide concern that is considered to be one of the most significant causes of global climate change. For this reason, CO<sub>2</sub> reduction is an urgent challenge particularly in the traffic and transportation sectors.

From this point of view, the diesel engine is one of the most promising practical power source options owing to its higher thermal efficiency, and much research has been conducted to steadily improve its performances.<sup>(e.g. 1-9)</sup> However, diesel engines emit more NO<sub>x</sub> and soot than gasoline engines and therefore require costly additional devices, such as emissions aftertreatment systems, high-pressure injection systems, EGR, and turbocharging systems to

Reprinted with permission from SAE paper No.2011-01-1393,  
© 2011 SAE International.

meet severe emissions regulations like the Euro 6 standard. This cost disadvantage is one reason preventing diesels from growing in popularity throughout the world. This study imposed the following hardware limitations to keep costs low: 1) no use of a de-NO<sub>x</sub> aftertreatment catalyst, 2) the use of a single stage turbocharger, not a two-stage turbocharger, 3) the use of a commercially available common rail injection system with a maximum injection pressure of up to 180 MPa. Under constraints 1) to 3), a new combustion concept was developed that can reduce NO<sub>x</sub> to less than half the level stipulated by the Euro 6 emissions standards in the NEDC (i.e., 40 mg/km or less) without deteriorating fuel consumption. This study constructed the basic idea of the concept, and the fundamental performance of the engine based on this concept was confirmed using a single-cylinder engine. Subsequently, more realistic feasibility tests such as full-load performance, and startability and emissions in cold conditions were conducted using a multi-cylinder engine.

## 2. Methodology

Critical engine hardware parameters impacting engine performance include the fuel injector specifications (diameter and number of nozzle orifices, spray umbrella angle, and the like), compression ratio, swirl ratio, and piston cavity configuration. The best combination of these parameter settings was explored to establish this novel combustion concept. In order to reach an optimal solution as fast as possible through numerous choices, this development utilized an in-cylinder visualization technique with an optically accessible engine,<sup>(10)</sup> 3D-CFD incorporating the KIVA code, and the UniDES<sup>(11)</sup> in-house code that performs a 0-dimensional cycle simulation for a comprehensive analysis, in addition to general engine tests.

Generally, a single cylinder engine is more convenient to use than a multi-cylinder engine due to its more precise control of engine conditions such as the EGR ratio, input fuel amount, intake pressure, and so on. However, it is not appropriate for more practical tests such as full torque, cold startability, or emissions. Therefore, both types of engines were used in this study. The specifications of the test engines are shown in **Table 1**. The conventional engine is the one used in the Toyota Avensis, which is an inline 4-cylinder engine with a displacement of 2.2 L. It is equipped with a common rail injection system. The new

combustion system proposed in this study is drastically changed from the conventional engine. It has a lower compression ratio, specially designed injectors with very small and numerous orifices, a lip-less shallow type piston cavity, and a very low swirl ratio using a new straight-port cylinder head. A schematic diagram of the single-cylinder engine is shown in **Fig. 1**. The engine is equipped with motor driven compressor to enable intake pressure to be set freely. A soot filter and cooler is attached to the exhaust gas recirculation (EGR) system to properly condition the EGR gas. A schematic diagram of the multi-cylinder engine is shown in **Fig. 2**. A low pressure loop (LPL) EGR system was added to the original Avensis engine, which has a conventional high pressure loop (HPL) EGR system. Cylinder pressure was measured by a piezoelectric pressure transducer. Combustion noise was measured by the 450 model AVL combustion noise meter. Soot was measured by the 415 model AVL smoke meter.

A schematic diagram of the optically accessible engine is shown together with the imaging system in **Fig. 3**.<sup>(10)</sup> It is a long-piston version of the single-cylinder engine with the same basic specifications such

**Table 1** Specifications of test engines.

	Conventional	Developed engine
Displacement [L]	0.557/cylinder	
Bore × stroke [mm]	86×96	
Compression ratio	15.8	14
Injector:		
Diameter [mm] × number	0.113×9	0.08×16
Umbrella angle [deg.]	155	140
Piston cavity type	Lip-bowl	Lip-less shallow
Intake port type	Helical	Straight
Swirl ratio	2.2	0.5

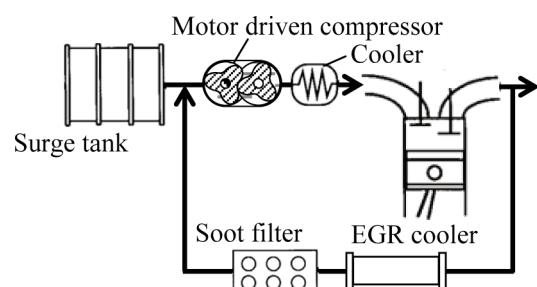


**Fig. 1** Schematic diagram of single-cylinder engine system used for basic tests.

as bore, stroke, and connecting rod length as the base engine. The spray and combustion images in the cylinder were taken by a high-speed video camera.

The primary models used in KIVA and UniDES<sup>(11)</sup> are summarized in **Table 2** and **3**, respectively. The calculated results are used in the later discussions.

### 3. Construction of New Combustion Concept

**Figure 4** shows the essence of the proposed combustion concept, which consists of three items. A specially designed injector, which can produce a low-penetrating and highly dispersed spray, is used in the concept. This spray is more advantageous for the utilization of PCCI. At the same time, a lower compression ratio and restricted in-cylinder flow motion are also employed. The purpose of the former is to improve full-load torque even when a low-

**Table 2** Primary models used in KIVA.

Physical process	Model
Droplet breakup/atomization	Surface-wave-growth <sup>(12)</sup>
Ignition	Shell model <sup>(13)</sup>
Combustion	Laminar-turbulence char. Time model <sup>(14)</sup>
Turbulence	RNG k- model <sup>(14)</sup>

**Table 3** Primary models used in UniDES.<sup>(11)</sup>

Physical process	Model
Spray formation	Multi-zone model
Air entrainment	Hiroyasu model <sup>(15)</sup>
Droplet size	Kawamura's equation <sup>(16)</sup>
Ignition	SHELL model <sup>(13)</sup>
Combustion	Laminar-turbulence char. Time model <sup>(14)</sup>
Turbulence	Ikegami model <sup>(17)</sup>
Heat-loss	Woschni model <sup>(18)</sup>

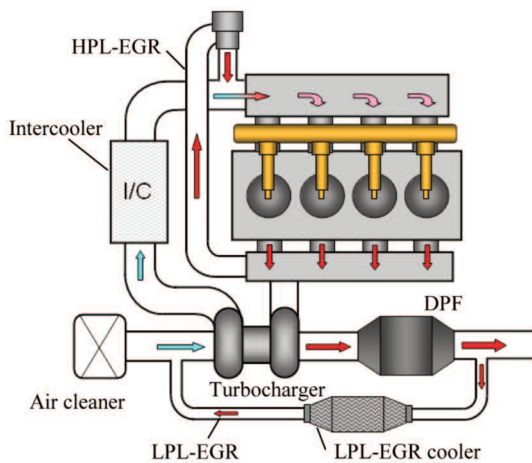


**Fig. 2** Schematic diagram of multi-cylinder engine system used for full-torque and cold startability tests.

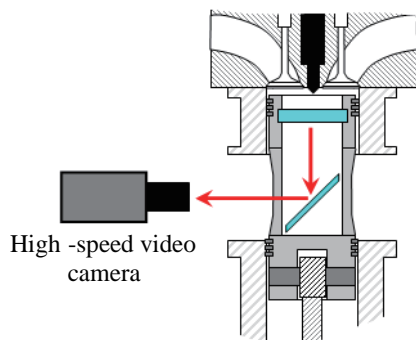


**Fig. 3** Schematic diagram of optically accessible engine with imaging system.

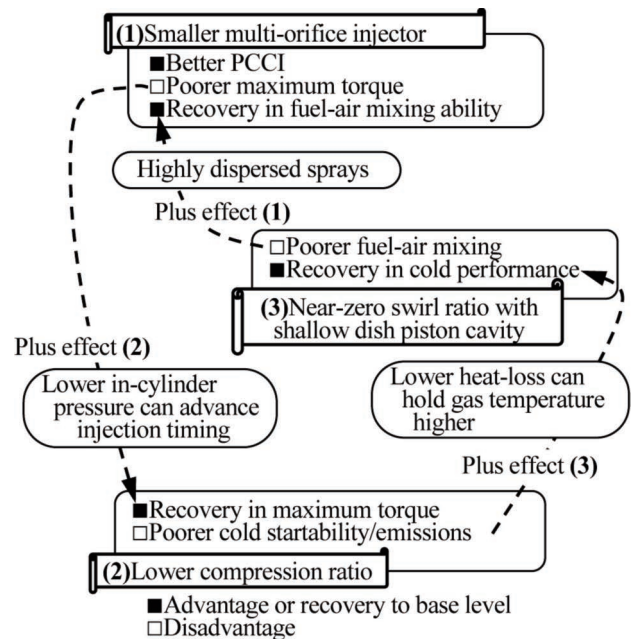


**Fig. 4** Essence of the proposed combustion concept, which maximizes synergy by mutual combinations of three items.

penetrating spray is used, and the latter is to reduce heat loss for better fuel economy and to recover engine performance in cold conditions even with the low compression ratio. The following sections will discuss in more detail the positive and negative effects of each of the three items, and how the negative effects of each were overcome.

### 3.1 Specially Designed Injector

Generally, PCCI helps to lower both NO<sub>x</sub> and soot emissions. However, as the engine speed and load become higher, the PCCI mixture become more heterogeneous due to the lack of time for fuel-air mixing, which has the effect of increasing emissions. In this case, advancing the injection timing further to secure enough mixing time would increase the amount of unburned hydrocarbons (HC) or cause oil dilution by much heavier impingement of the liquid spray onto the chamber wall. This is because the lower ambient pressure caused by the further advancement of the injection timing makes increases spray penetration and the lower temperature slows fuel evaporation. Therefore, the spray characteristics suitable for PCCI require both lower penetration for less wall-impingement and higher atomization for faster evaporation.

Previous reports have described the spray penetration (S) and the Sauter mean diameter (D<sub>32</sub>) in the following equations.<sup>(15,16)</sup>

$$S = 2.95 \times ((P_{cr} - P_a)/\rho_a)^{0.25} \times (d \cdot t)^{0.5} \quad (t > t_b) \quad [m] \cdots \cdots (1)$$

$$D_{32} = 72.36 \times (P_{cr} \times 10^{-6})^{-0.38} \times d \quad [m] \cdots \cdots (2)$$

where, P<sub>cr</sub>: common rail pressure [Pa], P<sub>a</sub>: ambient pressure [Pa], d: orifice diameter [m], t: time from injection start [s], t<sub>b</sub>: droplet breakup time [s]. D<sub>32</sub> can be used to identify the degree of spray atomization and a smaller D<sub>32</sub> means better atomization. The equations above imply the following: (1) a lower common rail pressure (P<sub>cr</sub>), is beneficial to lower penetration (S), but not to better atomization, (2) a smaller orifice diameter (D) is beneficial to both lower penetration and better atomization. Consequently, it was determined to use a very small orifice diameter of 80 micro-meters. On the other hand, such a small diameter requires a larger number of orifices to keep

the same level of fuel flow rate as with a conventional injector. Thus, the proposed injector uses numerous small-diameter orifices. In this paper, this PCCI-oriented injector is called the micro-multi injector (MMI). **Figure 5** shows a schematic comparison between conventional and MMI sprays to distinguish this spray concept more clearly.

**Figure 6** compares a conventional spray (left) and an MMI-produced spray (right) at an injection pressure of 130 MPa, photographed 0.5 ms from injection start. D<sub>32</sub> is 15 μm for the conventional spray and 12 μm for the MMI spray. This demonstrated that the MMI achieves a lower-penetrating and better-atomized spray, which is preferable for PCCI.

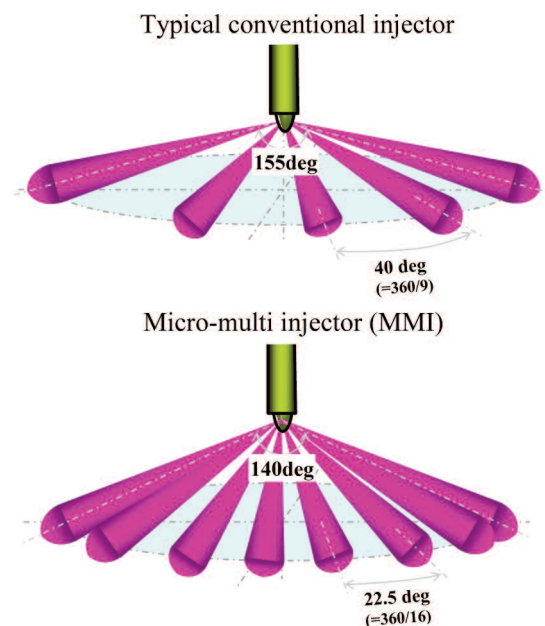


**Fig. 5** Schematic comparisons between conventional spray (top) and highly dispersed MMI spray (bottom).

φ 0.13 mm×10 (130 MPa)      φ 0.08 mm×22 (130 MPa)  
(Conventional, D<sub>32</sub> = 15 μm)      (Newly developed, D<sub>32</sub> = 12 μm)

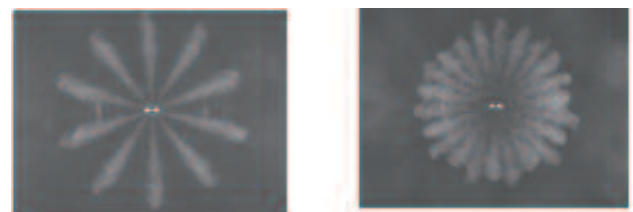


**Fig. 6** Comparison between conventional spray (left) and highly dispersed MMI spray (right) photographed at 0.5 ms.

**Figure 7** shows photographs of a combusting MMI-spray taken using the optically accessible engine from the bottom. Two cases were examined to investigate the effect of the number of orifices on the diffusive combustion of MMI spray. With a 22-orifice injector (left), the adjacent portions of the spray partially overlap each other, and seem to generate locally rich regions judging from the flame configurations. In contrast, in a 16-orifice injector (right), the spray portions are well arranged spatially with no interactions between the adjacent portions. In addition, the engine experiment also showed that the 16-orifice injector emitted less soot than the 22-orifice injector. Accordingly, the 16-orifice injector was adopted in this study.

The spray umbrella angle was selected in consideration of hydrocarbons in PCCI and soot in diffusive combustion. A narrower cone angle is beneficial to PCCI owing to less wall impingement of the spray by creating a longer distance to the wall. It is also advantageous to full-load torque, as discussed in the following section. Consequently, a 140-degree spray umbrella angle was adopted, compared to 155 degrees for a conventional engine.

### 3.2 Lower Compression Ratio

Generally, a highly dispersed and low-penetrating spray like the MMI-spray described above tends to generate more soot in diffusive combustion, which could lead to a serious torque reduction problem at full load. This study applied a lower compression ratio to recover full-load torque performance. **Figure 8** shows cylinder pressures and heat release rates of two cases with different compression ratios of 15 and 14. The

allowable maximum in-cylinder pressure ( $P_{max}$ ) is 16 MPa in this engine, and smoke at full load was also limited to an allowable level. The injection timing and input fuel quantity were independently adjusted so as not to exceed both the limitations of allowable  $P_{max}$  and smoke level. Since the lower compression ratio case creates lower compression-end pressure, the injection timing can be advanced further owing to the larger margin between  $P_{max}$  and the compression-end pressure. In addition, the combustion was completed earlier than in the case of the higher compression ratio, resulting in lower soot. Therefore, in spite of the low-penetrating spray, full-load torque can be recovered to the conventional level.

However, a lower compression ratio may worsen fuel economy. This section discusses the relationship between the compression ratio and thermal efficiency using the UniDES 0-dimensional in-house code.<sup>(11)</sup>

**Figure 9** shows a schematic overview of UniDES with

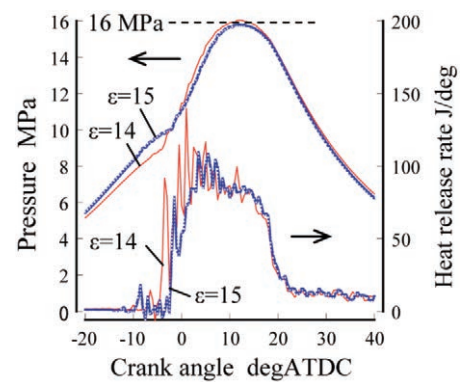


**Fig. 8** In-cylinder pressure and heat release rate with different compression ratios, while keeping maximum in-cylinder pressure at less than 16 MPa and smoke number at less than 0.8FSN at a full load of 2,000 rpm (measured).

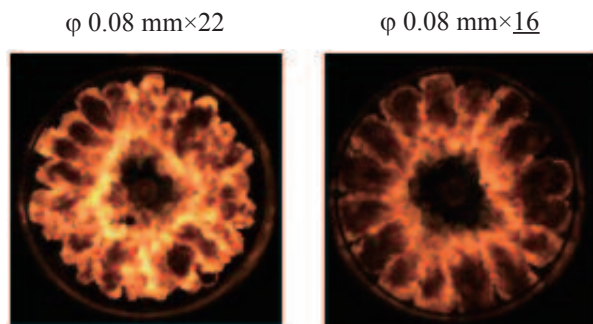


**Fig. 7** Effect of number of orifices on diffusive combustion, photographed from the bottom using optically accessible engine. (left: number of orifices = 22, right: 16)

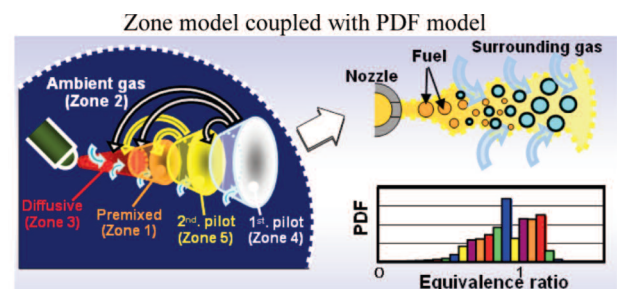


**Fig. 9** Overview of UniDES in-house code<sup>(11)</sup> with schematics of zone model and probability density function (PDF) model.

its primary models. Although UniDES is based on a 0-dimensional cycle simulation, it can reproduce the fuel-air mixing process closely by combining the originally proposed multi-zone and probability density function (PDF) models. It has been reported to accurately predict basic engine performance, such as indicated specific fuel consumption (ISFC), emissions, and combustion noise.<sup>(11)</sup> UniDES was used to estimate thermal efficiencies for various compression ratios with different injection timings. **Figure 10** shows a simulated example of heat release rates with changes in injection timings. It is supposed that UniDES can reasonably predict the transition of combustion characteristics based on injection timings, covering from PCCI-like combustion to diffusive combustion. **Figure 11** shows the simulation results for brake thermal efficiency and heat-loss ratio for

various compression ratios. The figure indicates that changes in compression ratio between 18 and 14 can hold brake thermal efficiency at almost the same level, just by selecting the appropriate injection timing. This is because even if the compression ratio is decreased within this range, the deterioration of the theoretical thermal efficiency can be canceled by reducing heat-loss. Consequently, a compression ratio of 14 was adopted in this study, which is the minimum ratio to keep the brake thermal efficiency at the same level as a conventional engine with an ordinary compression ratio.

Another advantage gained by a lower compression ratio is demonstrated in **Figs. 12** and **13**. Figure 12 shows the heat release rates with in-cylinder pressures for two cases of PCCI with different compression ratios of 14 and 15. Both cases were measured under

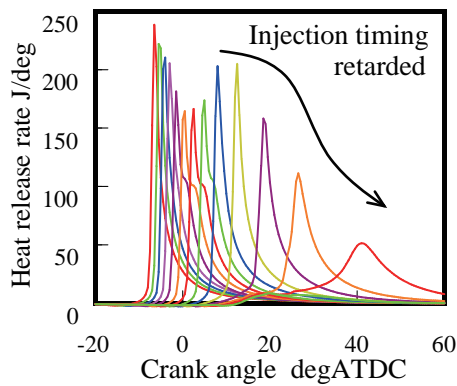


**Fig. 10** Example of heat release rates with different injection timings simulated by UniDES. (compression ratio: 16, IMEP: 0.7 MPa, EGR ratio: 0%)

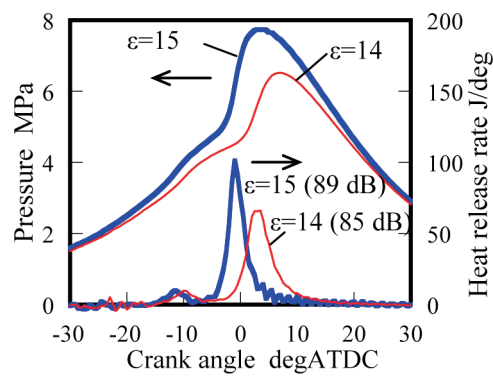


**Fig. 12** Effect of compression ratio on combustion characteristics of PCCI measured at same EGR ratio. (engine speed: 1,600 rpm, injection pressure: 130 MPa)

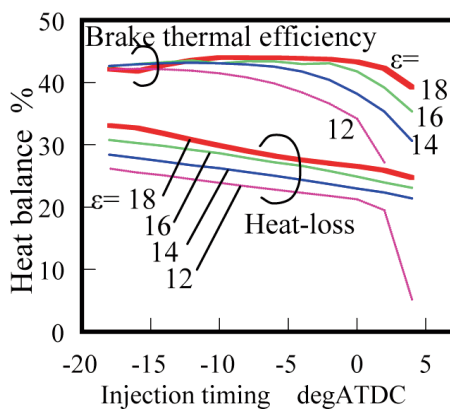


**Fig. 11** Brake thermal efficiency and heat-loss for various compression ratios simulated by UniDES. (engine speed: 1,200 rpm, injection pressure: 60 MPa)

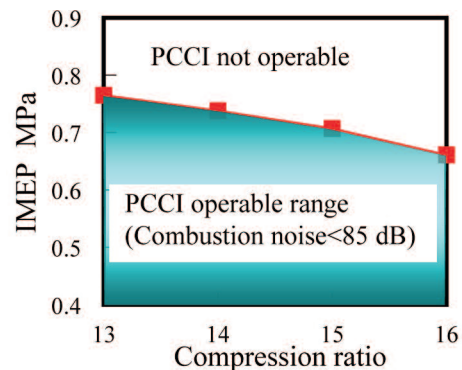


**Fig. 13** Maximum PCCI operable range in IMEP restricted to 85 dB of combustion noise simulated by UniDES. (engine speed: 1,600 rpm)

the same operating conditions, such as intake temperature, pressure, EGR ratio, and injected fuel quantity. Compared to the higher value, the ignition timing is retarded and the peak of heat release rate is lowered with the lower compression ratio. This is because a lower compression ratio creates both lower gas density and temperature during the combustion period, and it results in a slower chemical reaction rate. Since these experiments show that combustion noise is reduced by 4 dB in the lower case, the operable range of PCCI can be extended, since this is limited by the allowable combustion noise level. UniDES results predict that the PCCI-operable load can be extended by about 10% by decreasing the combustion ratio from 16 to 14, as shown in Fig. 13. Needless to say, this also means an overall reduction in NO<sub>x</sub> and soot emissions in the NEDC.

### 3.3 Very Weak In-cylinder Flow

Generally, an engine with a compression ratio of 14 would have poor cold-condition engine performance such as startability and unburned hydrocarbons. This study applied drastically lowered in-cylinder flow with a very low swirl port and lip-less shallow dish type piston cavity to recover cold-condition performance by lowering heat-loss.

**Figure 14** shows the compression-end gas temperatures (TDC-temperature) at idling engine speed (800 rpm) with changes in compression ratio (left) and swirl ratio (right) under cold engine conditions, as obtained using UniDES. Here, the base conditions are a compression ratio of 16 and a swirl ratio of 2.0. Gas temperatures were calculated

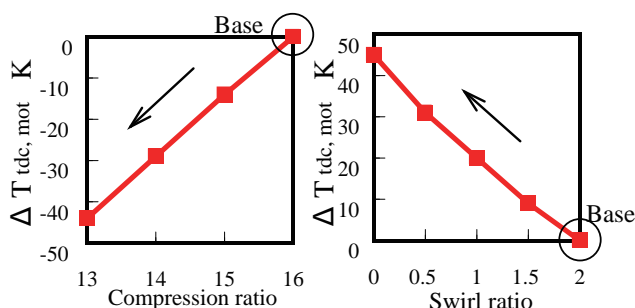


**Fig. 14** In-cylinder gas temperature at compression top dead center (TDC) at idling engine speed (800 rpm) with changes in compression ratio (left) and swirl ratio (right), simulated by UniDES for cold engine conditions.

considering the heat-loss model proposed by Woschni.<sup>(18)</sup> The intake gas and wall temperatures were set to  $-20$  degrees C. The left graph shows that the TDC-temperature is decreased by 30 degrees by lowering the compression ratio from 16 to 14. According to Woschni's heat loss model,<sup>(18)</sup> the heat transfer coefficient depends on in-cylinder swirl velocity. As a lower swirl motion reduces the heat transfer coefficient, the degree of heat-loss is reduced. Accordingly, the TDC-temperature increases with a lower swirl ratio, as the right side of the figure shows.

**Figure 15** was obtained by combining both the left and right graphs of Fig. 14. It shows the relationship of the compression ratio and swirl ratio with ignitability. The slanting line in Fig. 15 depicts the same TDC-temperature conditions as the base conditions (compression ratio: 16, swirl ratio: 2.0), and divides into two areas by its boundary line. The area above the boundary corresponds to a lower TDC-temperature condition, and the area below the boundary corresponds to a higher TDC-temperature condition. It means that the former has worse and the latter has better ignitability, respectively. Figure 15 indicates that the swirl ratio under a compression ratio of 14 should be reduced to less than 0.5 to achieve the same or better ignitability compared to the base engine conditions.

In order to make such a very low swirl ratio, a straight-port type cylinder head was developed instead of a conventional swirl-port head. The port shapes were modified using 3D-CFD, and the shape for achieving a swirl ratio of 0.5 was finally determined as shown in **Fig. 16**. The intake swirl ratio was measured experimentally using a vane type swirl

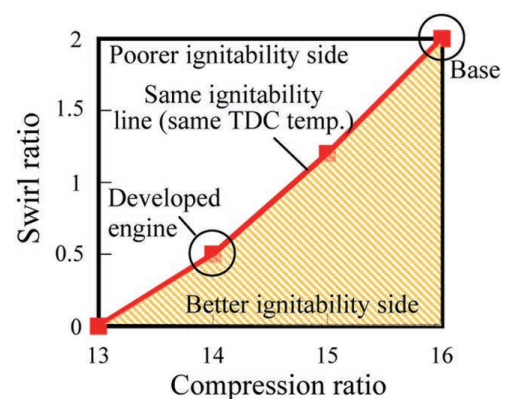


**Fig. 15** Relationship of compression ratio and swirl ratio with ignitability based on TDC temperature, obtained by combining Fig. 14 graphs.

meter.<sup>(19)</sup>

Additionally, the piston cavity shape was modified to a lip-less shallow dish type from the standard lip-bowl type, as compared in **Fig. 17**. A shallow piston cavity can suppress both swirl spin-up and squish flow induced by the piston motion. Such a weak in-cylinder gas motion can recover cold-condition engine performance under a low compression ratio to the conventional level.

Although a weak in-cylinder gas motion might lead to higher soot emissions due to slower fuel-air mixing, it should be noted that the highly dispersed MMI spray enables PCCI-dominant combustion in which the fuel-air mixing process is less dependent on in-cylinder flow. In this way, MMI compensates for the disadvantage of weak in-cylinder gas motion.

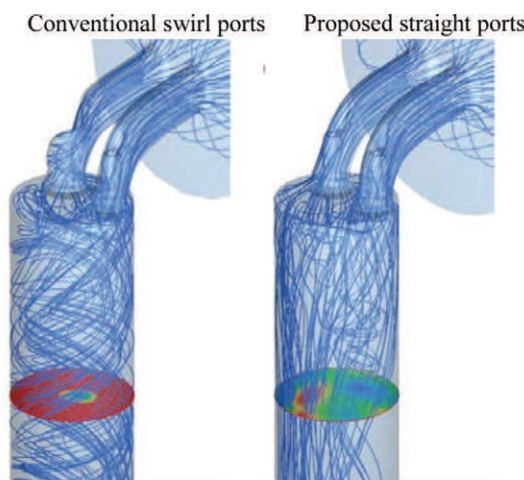


**Fig. 16** Intake port configurations. (left: used in conventional engine, right: proposed in the present study)

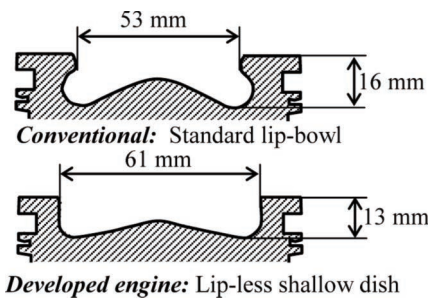


**Fig. 17** Piston cavity configurations. (top: used in conventional engine, bottom: proposed in the present study)

### 3.4 Synergy Effects

The key items of the proposed concept and their functional mutuality are summarized in **Fig. 18**. It features the following three items: (1) low-penetrating and highly dispersed spray using a specially designed injector with very small and numerous orifices, (2) a lower compression ratio, and (3) drastically restricted in-cylinder flow by means of very low swirl ports and a lip-less shallow dish type piston cavity.

Item (1) creates a more homogeneous air-fuel mixture with early fuel injection timings, while preventing wall-wetting, i.e., impingement of the spray onto the wall. In other words, this spray is suitable for PCCI operation, and can decrease both NO<sub>x</sub> and soot considerably when the utilization range of PCCI is maximized.

However, in diffusive combustion, especially at full load, a low-penetrating spray potentially causes higher soot emissions and results in lower maximum torque. In this case, item (2) is applied to recover full-load performance. The lower compression ratio enables diffusive combustion phasing to be advanced more with an earlier injection timing because of a larger margin between the compression-end pressure and the allowable maximum in-cylinder pressure. It has the effect of lowering soot emissions because enough time is created to oxidize soot before the end of the combustion period.

A lower compression ratio often leads to worse cold-condition engine performance aspects such as cold startability, unburned hydrocarbons, and white smoke. Item (3) is applied to compensate for such practical problems. Drastically weakened in-cylinder flow keeps

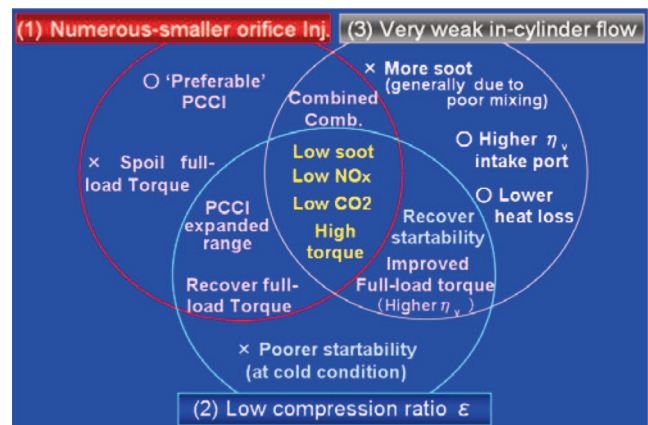


**Fig. 18** Schematic overview of the proposed new combustion concept.

the compression-end-temperature to the same level as a conventional engine with an ordinary compression ratio by decreasing heat-flux escaping through the chamber wall (i.e., heat-loss).

Although a weak in-cylinder gas motion might lead to higher soot emissions due to slower fuel-air mixing, it should be noted that the highly dispersed spray of item (1) enables PCCI-dominant combustion in which the fuel-air mixing process is less dependent on in-cylinder flow.

Furthermore, prompt fuel evaporation following the better atomization due to the smaller orifices of the MMI is also an effective way of improving cold-condition performance with a lower compression ratio. A straight-port head with high volumetric efficiency, which can take more air into the cylinder, is also effective at reducing soot emissions and consequently enhances full-load torque even with a low penetrating spray. In this way, these three items act mutually to compensate for each other's defects, while maximizing their advantages.

#### 4. Results and Discussions

##### 4.1 Fundamental Engine Performances at Partial Load

The fundamental engine performance of the proposed concept was tested using a single-cylinder engine. **Figure 19** shows the seven tested engine operating points, representing the New European Driving Cycle (NEDC).

**Figures 20 to 22** show the effects of the piston cavity type and swirl ratio on the indicated specific fuel consumption (ISFC), NO<sub>x</sub>, and smoke in mode 4, respectively. In mode 4, the engine runs in PCCI with

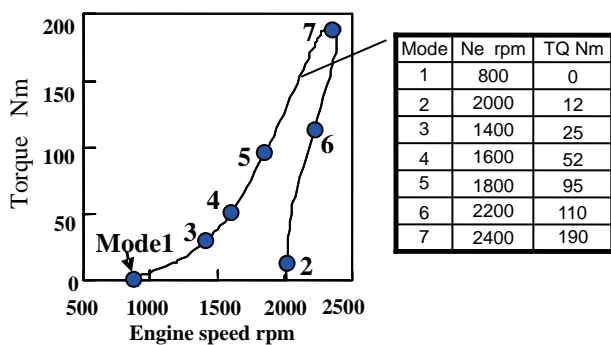


**Fig. 19** Engine operating points representing New European Driving Cycle (NEDC).

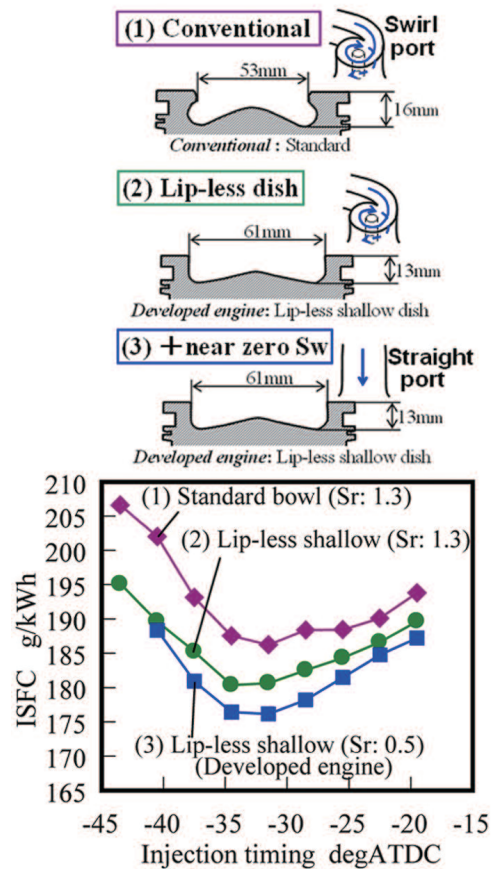


**Fig. 20** Effects of piston cavity configuration and swirl ratio (Sr) on ISFC with different injection timings in mode 4. (engine speed: 1,600 rpm, injection pressure: 130 MPa)

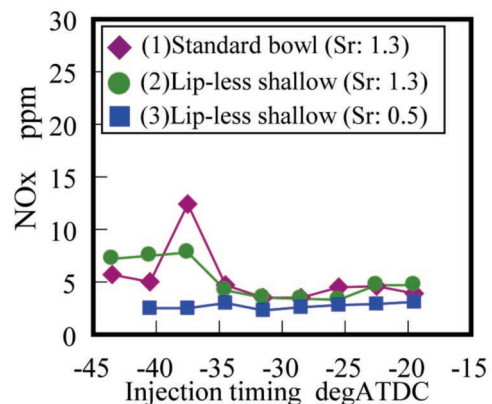


**Fig. 21** Effects of piston cavity configuration and swirl ratio (Sr) on NO<sub>x</sub> with different injection timings in mode 4. (engine speed: 1,600 rpm, injection pressure: 130 MPa)

a single injection at early timings. For various injection timings, the EGR ratio was tuned to keep a constant combustion noise of 87 dB. Three cases were examined. Case 1 used a standard bowl cavity with a swirl ratio of 1.3. Case 2 used a lip-less shallow dish with a swirl ratio 1.3. Case 3 used a lip-less shallow dish with a swirl ratio of 0.5. All cases used the same MMI conditions to distinguish only the in-cylinder swirl and squish flows. By changing the cavity from the standard bowl (case 1), to a lip-less shallow dish (case 2), ISFC is decreased by 3%. Furthermore, by reducing the swirl ratio to 0.5 (case 3), ISFC is decreased by 2%. In total, 5% improvement in ISFC was gained with the lower in-cylinder flow motion. As shown in Figs. 21 and 22, there are no large differences in NOx and smoke emissions between the three cases.

3D-CFD simulations with KIVA were conducted to understand the cause of these ISFC improvements. **Figure 23** shows the CFD results for overall heat-loss histories and the distribution of heat flux on the cavity wall surface. The figure indicates that in the developed engine, the heat transfer coefficient around the cavity edge is remarkably reduced by the modulation of both the cavity shape and the lower swirl ratio. Therefore, overall heat-loss is reduced by half. In this way, the process of the lower heat-loss and the resultant improvement in ISFC can be reasonably explained by 3D-CFD.

**Figure 24** compares total hydrocarbons (THC) and NOx emissions between the highly dispersed and low-penetrating spray (i.e., the MMI-spray) and the conventional spray in mode 4. The lip-less shallow

dish piston was used for the two cases. Data was collected by changing the injection timing. Side view spray-photographs for the two cases are superimposed on the right side of the figure. Both THC and NOx emissions are smaller with the MMI spray. This can be explained by the 3D-CFD results as shown in **Fig. 25** based on the spatial distributions of fuel vapor for the two cases. The conventional spray impinges heavily on the cavity sidewall due to its stronger penetration and generates a very fuel-rich region around the spray-wall impinging point. In contrast, the MMI spray prevents heavy spray-wall impingement due to its weaker penetration. Additionally, it is vaporized more promptly due to its better atomization. Both these factors can avoid the formation of a fuel-rich region around the wall. Consequently, THC generated by a rich mixture can be reduced more by lower locally rich

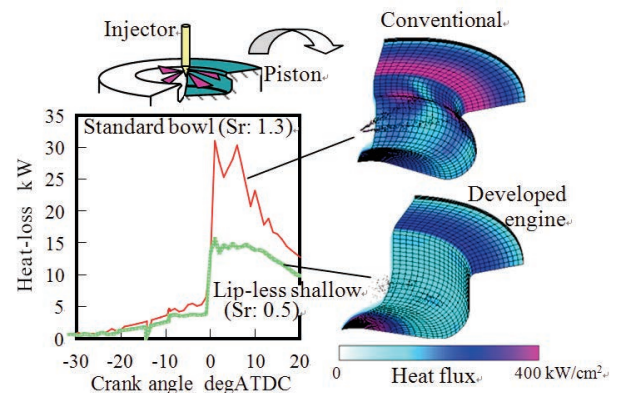


**Fig. 23** Overall heat-loss histories and distributions of heat flux for two cases: standard bowl cavity with swirl ratio (Sr) of 1.3 and lipless-shallow dish cavity with swirl ratio of 0.5 simulated by KIVA. (engine speed: 1,600 rpm, injection pressure: 130 MPa)

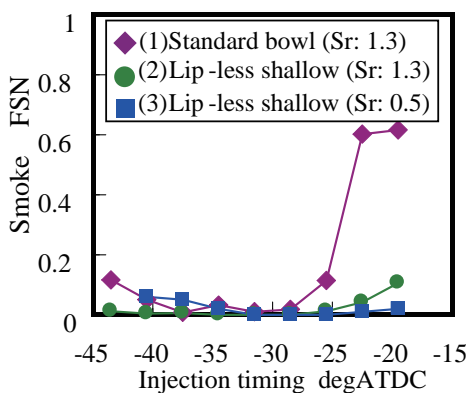


**Fig. 22** Effects of piston cavity configuration and swirl ratio (Sr) on smoke with different injection timings in mode 4. (engine speed: 1,600 rpm, injection pressure: 130 MPa)

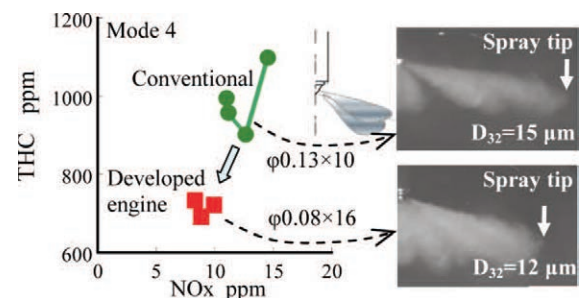


**Fig. 24** Effect of highly-dispersed spray on THC-NOx emissions of PCCI (left) and spray side-view photographs (right).

conditions under a larger EGR ratio, while also achieving lower NOx emissions. **Figure 26** compares ISFC and NOx emissions between the MMI and conventional sprays in the same engine conditions as Fig. 24. ISFC is better with the MMI-spray thanks to reducing the unburned fuel.

PCCI with a single injection cannot cover the whole engine operating range due to the limitation of combustion noise, as indicated in Fig. 13. At a high load around mode 7, multiple injection strategies were examined for both the proposed and the conventional engines instead of single-injection. **Figure 27** shows experimental results based on fuel mass flow rate

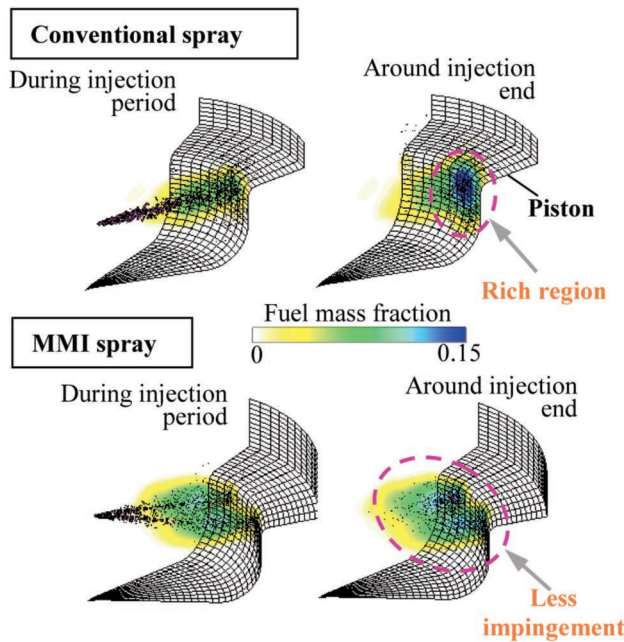


**Fig. 25** Spatial distributions of fuel vapor simulated by 3D-CFD. (top: conventional spray, bottom: MMI spray)

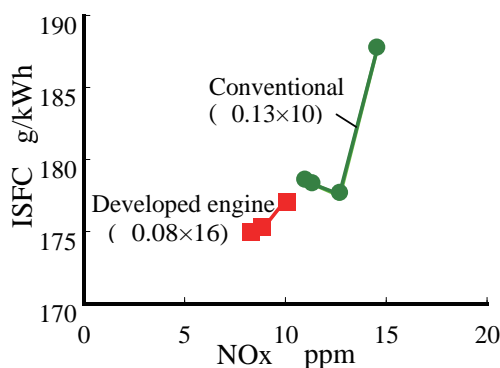
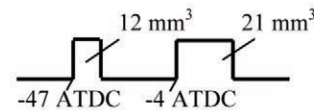


**Fig. 26** Effect of highly-dispersed spray on ISFC-NOx relationship. (same engine conditions as Fig. 21)

patterns for two cases using the conventional engine (case 1) and the developed new engine (case 2). In case 1, the fueling events consist of a pilot injection with a smaller fuel quantity and a main injection with a larger one. In case 2, the pilot injection timing can be more advanced and its quantity can be made considerably larger than in case 1. It should be noticed that the low-penetrating MMI spray, which can avoid fuel-wall impingement, enables such pilot injection with a larger quantity at an advanced injection timing. As shown in Fig. 27, case 2 completes combustion earlier than case 1. Generally, earlier combustion phasing would generate larger NOx emissions. However, the smoke-NOx trade-off curve is greatly improved in case 2, as shown in **Fig. 28**. **Figure 29** shows the relationship between ISFC and NOx in the same engine condition as Fig. 27. Case 2 has better ISFC than case 1 because the combustion phasing of case 2 is relatively advanced and the degree of constant volume is improved.

3D-CFD by KIVA was conducted to investigate the causes of this soot-NOx trade-off improvement at high load. To clarify the difference in in-cylinder gas conditions of the two cases, the 3D-CFD results were

**Case 1:** Conventional engine with standard injection



**Case 2:** Developed engine with advanced injection timings

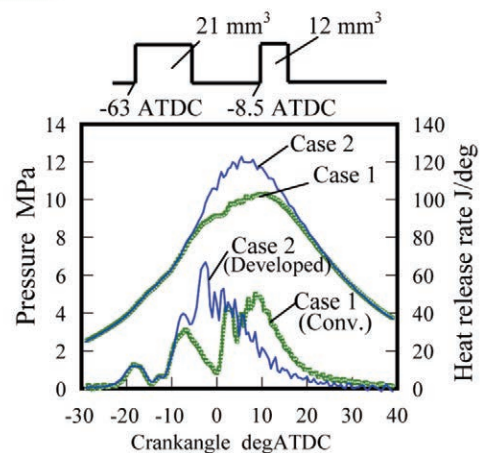


**Fig. 27** Injected fuel mass flows rates with injection timings (top) and histories of pressure and heat release rate (bottom) for two cases: the conventional engine (case 1) and the developed engine (case 2) at a high load. (engine speed: 2,600 rpm, torque: 130 Nm)

coupled with an equivalence ratio ( $\phi$ )-temperature (T) map, on which soot and NO<sub>x</sub> formation areas are depicted from reference.<sup>(20)</sup> In **Fig. 30**, the gas conditions of  $\phi$  and T at each computational cell are superimposed on the  $\phi$ -T map, marked in green for case 1 and in blue for case 2. In case 1, diffusive combustion from the second injection dominantly proceeds within the whole cavity. Some plots in case 1 cross into the soot formation area and some are in the NO<sub>x</sub> formation area. In contrast, in case 2, PCCI combustion from the first injection dominantly proceeds in the outer side of the chamber, widely ranging from the squish area up to around the cavity side wall. At the same time, minor diffusive combustion from the second injection occurs at the inner side of the cavity. In other words, major PCCI can consume the oxygen at the outer side of the chamber and the minor diffusive combustion consumes the oxygen at the inner side. This means that

case 2 can use the whole of the oxygen in the cylinder. Overall, case 2 achieves a more diluted fuel-air mixture, and the plots for case 2 are shifted toward the leaner side of  $\phi$  and the lower temperature side, compared to case 1. In this way, the gas conditions of case 2 can escape from the soot and NO<sub>x</sub> formation areas, and the soot-NO<sub>x</sub> trade-off is considerably improved even at higher loads. This multiple injection strategy with this new engine can be called combined combustion because it uses a combination of PCCI and diffusive combustion very effectively.

To express the overall engine performance in the NEDC, **Fig. 31** shows the NO<sub>x</sub>-CO<sub>2</sub> trade-off curves of the conventional and developed engines, which

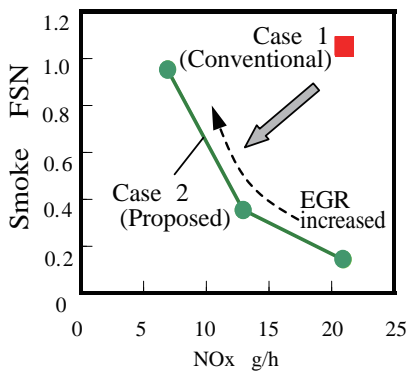


**Fig. 28** Trade-off between NO<sub>x</sub> and smoke for two cases: with the conventional engine and the developed engine at a high load. (same conditions as Fig. 27)

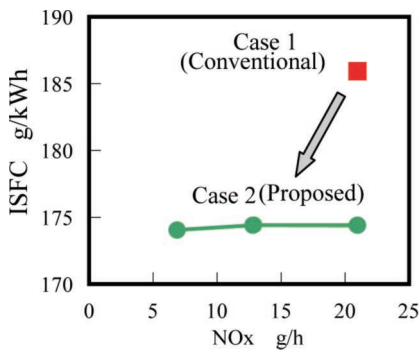


**Fig. 29** Relationship between NO<sub>x</sub> and ISFC for two cases: with the conventional engine and the developed engine at a high load. (same conditions as Fig. 27)

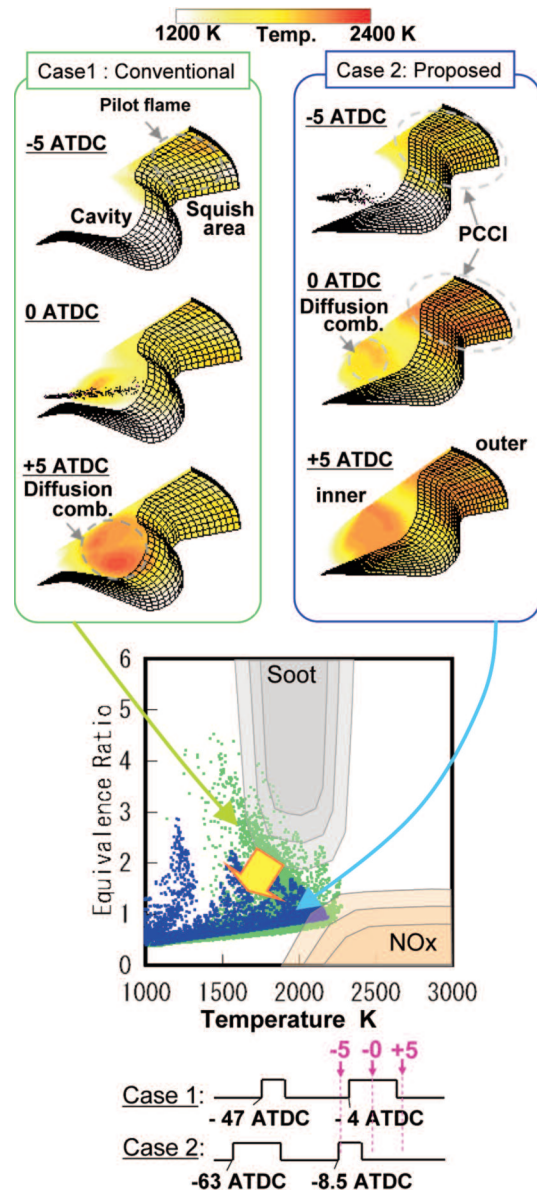


**Fig. 30**  $\phi$ -T map analysis combined with 3D-CFD results under same engine conditions as Fig. 27.

were obtained based on the experimental data at the representative mode points from 1 to 7. NO<sub>x</sub> in the developed engine can be decreased to less than one-fourth the level of the conventional engine, which is tuned for the Euro 4 emission standards, without any deterioration in CO<sub>2</sub>. In case A in Fig. 31, in which the PCCI operation range is maximized as much as combustion noise permits, NO<sub>x</sub> can reach a level of 30 mg/km level, which is less than half of the Euro 6 standard. In case B with limited PCCI operation, CO<sub>2</sub> can be decreased further by reducing unburned HC and CO. In any case, it has been confirmed using a single-cylinder engine that the developed engine can offer a remarkable reduction in NO<sub>x</sub> with better CO<sub>2</sub> than the conventional engine.

#### 4.2 Full-load and Cold-condition Performance

More realistic feasibility tests such as full-load performance and startability and emissions in cold conditions were conducted using a multi-cylinder engine.

Figure 32 shows engine torque and brake specific fuel consumption (BSFC) at full loads for various

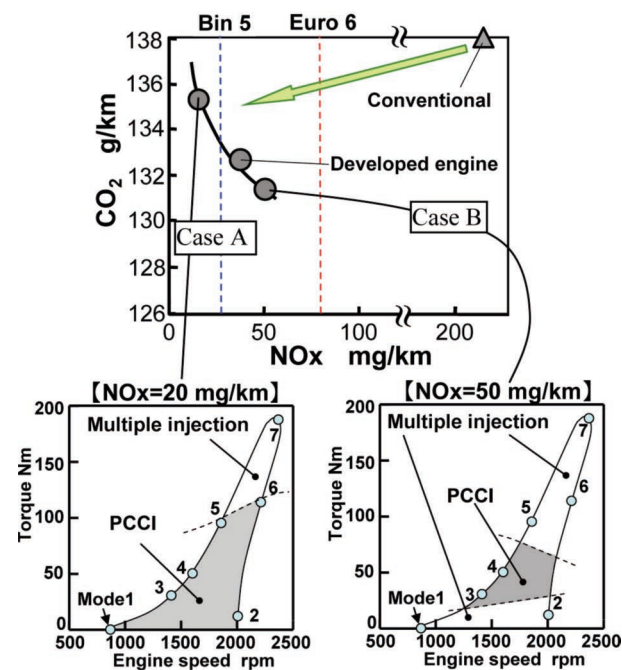


Fig. 31 Trade-off curve between CO<sub>2</sub> and NO<sub>x</sub> emissions in NEDC (top) obtained from the performance at 7 engine operating points, and combustion-type classifications on engine-speed/torque map of two representative calibrations: case A for lower NO<sub>x</sub> and case B for lower CO<sub>2</sub> (bottom).

engine speeds. Full-load torque is defined as the maximum torque at a fuel quantity that does not exceed an allowable smoke level. In other words, a small-orifice injector like MMI, which potentially generates more smoke in diffusion combustion, might reduce the full-load torque. As described in the proposed concept, lowering the compression ratio is more advantageous to improving full-load torque thanks to the reduced soot due to advancing the injection timing under an allowable in-cylinder pressure. Therefore, this concept using a combination of MMI and a lower compression ratio is expected to have equivalent torque to conventional engines at full loads. Actually, as shown in Fig. 32, it can offer the same torque at 3,600 rpm and 10% higher torque at 1,400 rpm and 2,000 rpm. Furthermore, the BSFC of this concept is, as a whole, better compared to the conventional engine thanks to the lower heat-loss created by the weaker in-cylinder flow.

3D-CFD analyses with KIVA were conducted to provide another insight into the mechanism for such a full-load torque improvement. Figure 33 shows the mixture formation processes of the conventional (left) and the developed engines (right), simulated by KIVA. In the conventional engine, during the compression stroke, a squish flow is induced and rotates with a clockwise motion, while influenced by the centrifugal force in the swirl motion, as drawn in orange at -7 ATDC. In the expansion stroke, the squish flow turns to rush toward the squish area and acts to push away fuel spray to the squish area. In this situation, the fuel spray needs strong penetration to prevent it from being taken away with the squish flow. With a strong

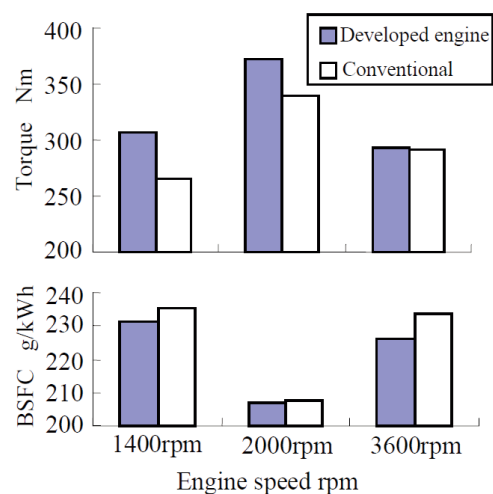


Fig. 32 Full-torque performance of multi-cylinder engine.

penetration, the spray and mixture rotates in the cavity first, and then leaves for the squish area, as shown in the pictures at 10 and 40 ATDC. Such spray and mixture movements, which enable the use of both the air of the cavity and the squish area can decrease soot, and resultantly improve full-load torque. This is a reason why a higher spray penetration with a high injection pressure or large nozzle orifice size is more beneficial to full-load performance. In contrast, in the new concept (right side in Fig. 33), the squish flow is weakened by the lip-less shallow dish and has a counterclockwise motion owing to the smaller influence of centrifugal force due to the very low swirl ratio, as drawn in orange at -7 ATDC. Additionally, because the MMI is designed to have a narrower cone angle compared to the conventional spray, the squish flow direction eventually coincides with the spray direction. In other words, unlikely the conventional case, there is no conflicting motion between the squish and the spray flows, which go together from the cavity toward the squish area, as shown in the pictures at 10 and 40 ATDC. Thus, in spite of the low-penetrating spray of MMI, the sprayed fuel can mix both the air of the cavity and the squish area, resulting in lower soot. This is another reason why the concept with MMI can also satisfy the full-load performance.

Finally, cold-condition tests were conducted using the multi-cylinder engine. **Figure 34** shows the temporal changes in engine speed and total hydrocarbons from engine start at an ambient temperature of 0 degrees C. It was confirmed that

although the new concept uses a very low compression ratio, both engine startability and total hydrocarbons are at the almost same level as the conventional engine thanks to lower heat-loss due to the very weak in-cylinder flow motion.

**Figure 35** shows the total hydrocarbons at a high altitude of 3,000 m at idling engine speed. It indicates a slightly better result than the conventional engine.

3D-CFD was conducted to understand the effect of the dispersed MMI spray on the ambient gas temperature at an idling engine speed. **Figure 36**

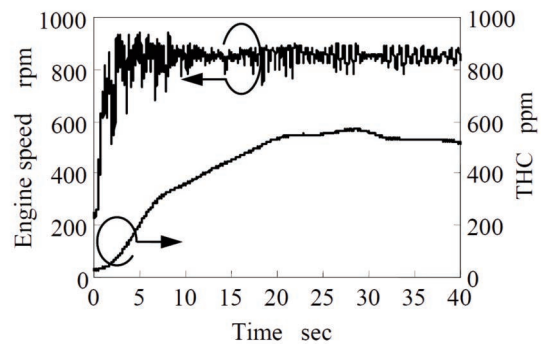


**Fig. 34** Temporal changes in engine speed and total hydrocarbons from engine start under low temperature conditions. (ambient air temperature: 0 degrees C)

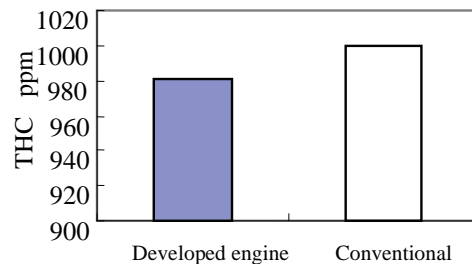


**Fig. 35** Total hydrocarbons at high altitude of 3,000 m at idling engine speed.

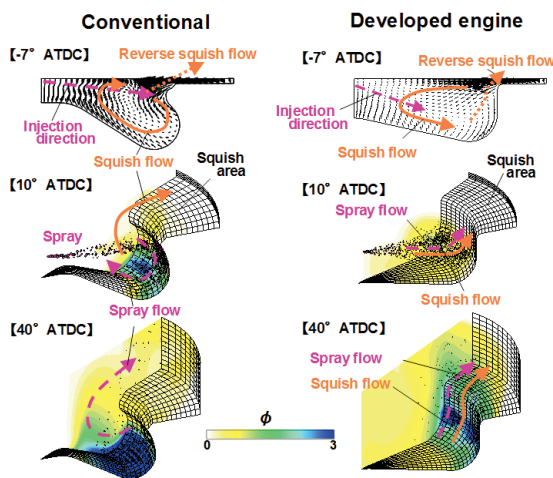


**Fig. 33** Mixture formation processes simulated by 3D-CFD at full-torque. (engine speed: 2,000 rpm)

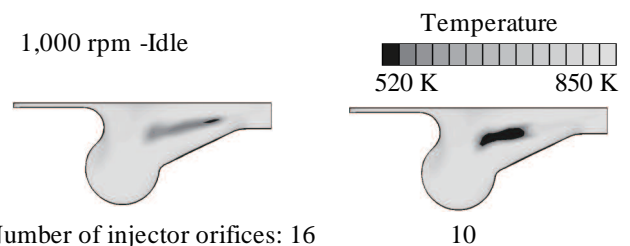


**Fig. 36** Temperature distribution for two cases: 10 and 16 orifices at 3° BTDC simulated by STAR-CD.

shows the results simulated by STAR-CD ver. 3.26. The sub-models that were used, such as fuel atomization, ignition, and combustion, are listed in references 14 and 15. The figure indicates that the use of numerous orifices helps to avoid excessive local-cooling of the latent heat of evaporation. Consequently, the surrounding gas temperature around the spray is kept higher before ignition, and ignitability and the succeeding combustion stability can be improved. It is noticeable that MMI also helps to solve such cold-condition problems, as well as the very weak in-cylinder flow motion.

## 5. Summary/conclusions

In this study, the basic idea of a new combustion concept was proposed and its novel performance aspects were demonstrated using a single-cylinder engine. Additionally, more realistic feasibility tests such as full-load performance and startability and emissions under cold conditions were examined using a multi-cylinder engine. Based on the results obtained, the following conclusions are made.

- A specially designed injector called the micro-multi injector (MMI) can create a good trade-off between hydrocarbons and NO<sub>x</sub> emissions in PCCI operation, thanks to generating a more homogenous mixture.
- Lowering the compression ratio to 14 can achieve the same or higher full-load torque than the conventional engine, even when the very small orifice MMI is used.
- Drastically lowering in-cylinder flow by the use of a straight-port head and lip-less shallow dish piston can decrease heat-loss through the combustion chamber wall. Consequently, cold-condition performance such as ignitability and unburned hydrocarbons are not inferior to the conventional engine in spite of the lower compression ratio of 14, and fuel economy is also improved with lower heat-loss.
- The PCCI-operable range can be extended to a higher load by combining MMI and the low compression ratio.
- In higher loads over the PCCI-operable range, combining PCCI and diffusive combustion by a multiple-injection strategy can improve the trade-off between NO<sub>x</sub> and smoke emissions.
- Consequently, NO<sub>x</sub> emissions in the New European Driving Cycle (NEDC) can be reduced drastically to less than 1/4 of the level of the conventional engine, or less than half of the Euro 6 standard, without deteriorating fuel consumption, full-load torque, or

cold-condition performance.

## Acknowledgments

The authors would like to gratefully acknowledge the valuable discussions with and advice from Dr. Makoto Koike and Dr. Kiyomi Nakakita of Toyota Central R&D Labs., Inc. and to express their gratitude to Mr. Terutoshi Tomoda and Mr. Yasuo Sato of Toyota Motor Corporation for their considerable cooperation with the engine experiments. Finally, the authors would like to note the substantial contribution of Mr. Yoshitaka Takeuchi at Toyota Industries Corporation in the development of the new engine cylinder head used in this work.

## References

- (1) Minato, A., et al., "Investigation of Premixed Lean Diesel Combustion with Ultra High Pressure Injection", *JSAE Proceedings* (in Japanese), No. 69-04 (2004), pp. 25-30.
- (2) Aoyagi, Y., et al., "Diesel Combustion and Emission Study by Use of High Boost and High Injection Pressure in Single-cylinder Engine - The Effects of Boost Pressure on Thermal Efficiency and NO<sub>x</sub>", *JSAE Proceedings* (in Japanese), No. 46-03 (2003), pp. 11-16.
- (3) Wakisaka, Y., Hotta, Y., Inayoshi, M., Nakakita, K., et al., "Emissions Reduction Potential of Extremely High Boost and High EGR Rate for an HSDI Diesel Engine and the Reduction Mechanisms of Exhaust Emissions", *SAE Tech. Paper Ser.*, No. 2008-01-1189 (2008).
- (4) Epping, K., Aceves, S., Bechtold, R. and Dec, J., "The Potential of HCCI Combustion for High Efficiency and Low Emissions", *SAE Tech. Paper Ser.*, No. 2002-01-1923 (2002).
- (5) Neely, G. D., Sasaki, S. and Leet, J. A., "Experimental Investigation of PCCI-DI Combustion on Emissions in a Light-duty Diesel Engine", *SAE Tech. Paper Ser.*, No. 2004-01-0121 (2004).
- (6) Kokjohn, S. L., Hanson, R. M., Splitter, D. A. and Reitz, R. D., "Experiments and Modeling of Dual-fuel HCCI and PCCI Combustion Using In-cylinder Fuel Blending", *SAE Tech. Paper Ser.*, No. 2009-01-2647 (2009).
- (7) Noehre, C., Andersson, M., Johansson, B. and Hultqvist, A., "Characterization of Partially Premixed Combustion", *SAE Tech. Paper Ser.*, No. 2006-01-3412 (2006).
- (8) Hou, D., Zhang, H., Kalish, Y., Lee, C.-f. F. and Cheng, W. L., "Adaptive PCCI Combustion Using Micro-variable Circular-orifice (MVCO) Fuel Injector - Key Enabling Technologies for High Efficiency Clean Diesel Engines", *SAE Tech. Paper*

- Ser., No. 2009-01-1528 (2009).
- (9) Ickes, A. M., Assanis, D. N. and Bohac, S. V., "Load Limits with Fuel Effects of a Premixed Diesel Combustion Mode", *SAE Tech. Paper Ser.*, No. 2009-01-1972 (2009).
  - (10) Fuyuto, T., Akihama, K., Fujikawa, T. and Nakakita, K., "Diesel In-cylinder Measurement Technique Using a Multi-direction Optically Accessible Engine", *Journal of Environment and Engineering*, Vol. 5, No. 1 (2010), pp. 72-83.
  - (11) Inagaki, K., Ueda, M., Mizuta, J., Nakakita, K., et al., "Universal Diesel Engine Simulator (UniDES)", *SAE Tech. Paper Ser.*, No. 2008-01-0843 (2008).
  - (12) Reitz, R. D., "Modeling Atomization Processes in High-pressure Vaporizing Sprays", *Atomization Spray Technol.*, Vol. 3, No. 4 (1987), pp. 309-337.
  - (13) Halstead, M., Kirsh, L. and Quinn, C., "The Autoignition of Hydrocarbon Fuels at High Temperatures and Pressures - Fitting of a Mathematical Model", *Combust. Flame*, Vol. 30 (1977), pp. 45-60.
  - (14) Kong, S.-C., Han, Z. and Reitz, R. D., "Modeling Engine Spray Combustion Processes", *Recent Advances in Spray Combustion: Spray Combustion Measurements and Model Simulation* (1996).
  - (15) Hiroyasu, H. and Arai, M., "Fuel Spray Penetration and Spray Angle in Diesel Engine", *JSAE Transaction* (in Japanese), No. 21 (1980), pp. 5-11.
  - (16) Kawamura, K. and Saito, A., *The 2nd Atomization Symposium* (1993), pp. 115-120.
  - (17) Ikegami, M., Shioji, M. and Koike, M., "A Stochastic Approach to Model the Combustion Process in Direct-injection Diesel Engines", *20th Symposium (International) on Combustion* (1984), pp. 217-224., The Combustion Institute.
  - (18) Sihling, K. and Woschni, G., "Experimental Investigation of the Instantaneous Heat Transfer in the Cylinder of a High Speed Diesel Engine", *SAE Tech. Paper Ser.*, No. 790833 (1979).
  - (19) Pischinger, F., "Entwicklungsarbeiten von Einem Verbrennungssystem fuer Fahrzeugdieselmotoren", *ATZ*, Jg.65, Nr. 1 (1963), pp. 43-46.
  - (20) Akihama, K., Takatori, Y., Inagaki, K., Sasaki, S. and Dean, A. M., "Mechanism of the Smokeless Rich Diesel Combustion by Reducing Temperature", *SAE Tech. Paper Ser.*, No. 2001-01-0655 (2001).
  - (21) Patterson, M. A. and Reitz, R. D., "Modeling the Effects of Fuel Spray Characteristics on Diesel Engine Combustion and Emissions", *SAE Tech. Paper Ser.*, No. 980131 (1998).
  - (22) Kong, S.-C., Han, Z. and Reitz, R. D., "The Development and Application of a Diesel Ignition and Combustion Model for Multidimensional Engine Simulations", *SAE Tech. Paper Ser.*, No. 950278 (1995).

---

**Kazuhisa Inagaki**

Research Field:

- Diesel Engine Combustion

Academic Degree: Dr.Eng.

Academic Societies:

- The Japan Society of Mechanical Engineers

- Society of Automotive Engineers of Japan

Awards:

- Outstanding Technical Paper Award of JSAE, 2004, 2005, 2009, 2010 and 2012

- SAE 2003 Harry LeVan Horning Memorial Award, 2004

- Best Presentation Award of JSAE, 2013




---

**Jun'ichi Mizuta**

Research Field:

- Diesel Engine Combustion

Academic Society:

- Society of Automotive Engineers of Japan

Awards:

- Outstanding Technical Paper Award of JSAE, 1997, 2010 and 2012




---

**Takayuki Fuyuto**

Research Field:

- Engine Combustion

Academic Societies:

- The Japan Society of Mechanical Engineers

- Society of Automotive Engineers of Japan

- Combustion Society of Japan

Awards:

- Encouragement Award, Combustion Society of Japan, 2009

- Outstanding Technical Paper Award of JSAE, 2009

- Outstanding Presentation Award of JSAE, 2011




---

**Takeshi Hashizume\***

Research Field:

- Development of Diesel Engine Combustion System

Academic Degree: Dr.Eng.

Academic Societies:

- The Japan Society of Mechanical Engineers

- Society of Automotive Engineers of Japan

Awards:

- Encouragement Award of JSME, 2000

- Outstanding Technical Paper Award of JSAE, 2012



---

**Hirokazu Ito\***

Research Field:

- Diesel Combustion

Academic Society:

- Society of Automotive Engineers of Japan

Award:

- Outstanding Technical Paper Award of JSAE, 2012



---

**Hiroshi Kuzuyama\*\***

Research Field:

- Diesel Engine Combustion

Academic Societies:

- Society of Automotive Engineers of Japan
- The Japan Society of Mechanical Engineers

Award:

- Outstanding Technical Paper Award of JSAE, 2012



---

**Tsutomu Kawae\*\***

Research Field:

- Diesel Engine Combustion

Academic Societies:

- Society of Automotive Engineers of Japan
- The Japan Society of Mechanical Engineers



---

**Masaaki Kono\*\*\***

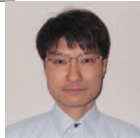
Research Fields:

- Diesel Engine Combustion
- SI Engine Combustion

Academic Degree: Dr.Eng.

Academic Society:

- Society of Automotive Engineers of Japan



---

\*Toyota Motor Corporation  
\*\*Toyota Industries Corporation  
\*\*\*NIPPON SOKEN, INC.